Presented at the Workshop on Position-Sensitive Detection of Thermal Neutrons
Institut Laue-Langevin, Grenoble, October 11-12, 1982

SPATIAL RESOLUTION OF NEUTRON-POSITION SCINTILLATION DETECTORS

M.G. Strauss, R. Brenner, H.P. Chou, A.J. Schultz and C.T. Roche

Argonne National Laboratory,

Argonne, Illinois, U.S.A.

1. INTRODUCTION

An Intense Pulsed Neutron Source (IPNS) was recently built at Argonne. From the point of view of neutron detection a pulsed source has two characteristics which are basically different from those of a steady-state source such as a reactor:

1) Broad spectrum of neutron energies in which a greater fraction of the flux is in the epithermal range.
2) High instantaneous neutron flux.

A detector to be used with a pulsed source should therefore have:

1) High neutron detection efficiency extending to epithermal energies.
2) High instantaneous count-rate capability.

In response to these requirements a new neutron position-sensitive detector was developed (1). The detector is comprised of an array of photomultiplier tubes coupled to a thin ^{6}Li-glass scintillator. The principle of operation is similar to that of the Anger gamma-ray camera (2) used in nuclear medicine.

In neutron scattering experiments the direction and the intensity of the scattering vectors are of principal importance. High precision measurements require high angular resolution. For a given angular resolution, high detector spatial resolution permits shorter detector-to-sample distance, and therefore a given size detector subtends a larger solid angle about the sample. In addition, the peak-to-background ratio is directly proportional to the spatial resolution. Thus having

detectors with high resolution reduces the required data collection time.

In this paper we describe the operation and performance of the detector, examine the parameters which affect the spatial resolution, report on resolution measurements and calculations, and discuss various means which can lead to improved resolution.

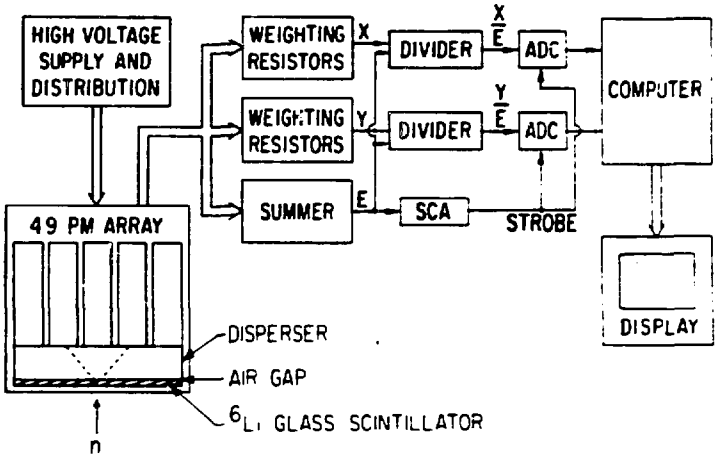

Fig. 1. Basic operation of neutron-position scintillation detector. The output from each photomultiplier (PM) is resistor weighted according to its X and Y coordinates. The normalized sums of the weighted signals give the centroid (X/E, Y/E) of the scintillation light cone.

2. NEUTRON-POSITION SCINTILLATION DETECTOR

The basic neutron-position scintillation detector consists of an array of photomultiplier tubes (PMTs) viewing a 1-2 mm thick ^{6}Li-glass scintillator (Fig. 1). In the recent version of the detector we used a 7x7 array of square (3) PMTs (each 51x51 mm^2) with a 30x30 cm^2 scintillator. The scintillator is coupled to the PMT array via a light disperser. The disperser spreads the scintillation light thereby permitting the determination of the location of the neutron interaction in the scintillator by interpolation between PMT centers. The front layer of the disperser consists of a boron containing glass (pyrex) separated from the scintillator by a thin air gap (<0.1 mm). The boron glass is optically coupled to a layer of plexiglass which in turn is optically coupled to the PMTs windows. The boron glass is used to shield the glass scintillator from neutrons which scatter back from the plexiglass and/or other structure.

The location of a neutron interaction in the scintillator is obtained by determining the centroid of the light cone received by the PMTs. The output from each PMT is resistor weighted according to its X and Y coordinates (Fig. 1). The

addition of the weighted signals from each axis represents the sum of the X and Y moments. Division of these by the unweighted sum of all the PMT signals E, produces the normalized coordinate signals (X/E, Y/E) of the neutron position of interaction in the detector. The normalization provides for coordinate signals which are independent of the amplitude of E. The coordinate signals are digitized by the analog-to-digital converter (ADC) and processed by the computer. The ADC are gated by the single channel analyzer (SCA) whose window is set to bracket the neutron peak (FWHM = 12-15%) thereby rejecting the γ-ray background.

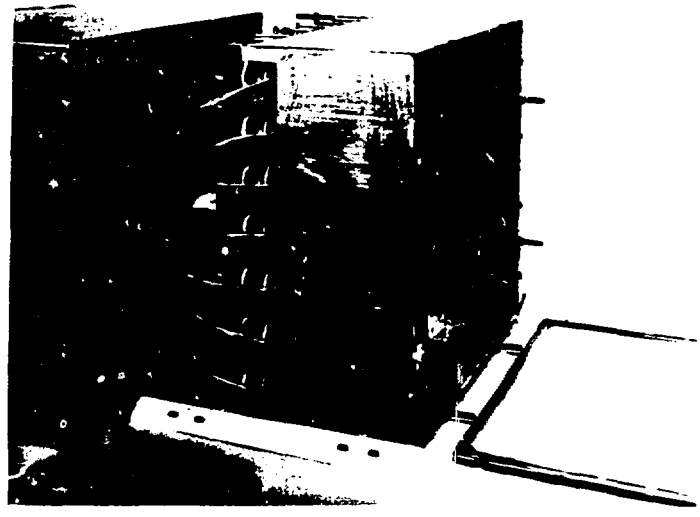

Fig. 2. Neutron-position scintillation detector consisting of an array of 7x7 square photomultiplier tubes (51x51 mm^2) coupled to a 30x30 cm^2 glass scintillator (shown detached).

An exploded view of the detector is shown in Fig. 2. The scintillator glass, backed by a diffusing Al_2O_3 powder reflector, is shown detached on the bottom. An array of square PMTs which are butted against each other collect more of the scintillation light than round PMTs. The PMTs are spring loaded to assure close optical coupling to the disperser. This design combines efficiency with simplicity of construction.

The above detector is incorporated in a single crystal diffractometer (4) in use at IPNS. A plot of a Laue pattern for a crystal of $K_{0.26}WO_6$ obtained from an experiment is shown in Fig. 3. The intensities are summed over a wavelength range of 1.0 to 3.0 $\mathring{A}$. All the Bragg peaks, including a number of satellite peaks, are completely resolved.

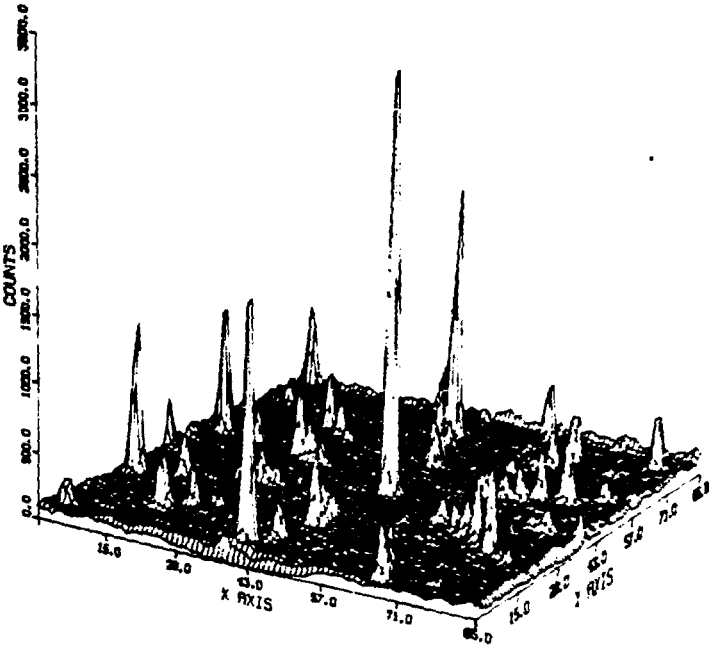

Fig. 3. Laue pattern for a crystal of $K_{0.26}WO_6$ obtained with a single crystal diffractometer in which the detector shown in Fig. 2 is incorporated. The intensities are summed over a wavelength range of 1.0-3.0 Å.

The salient features of a position-sensitive scintillation detector are:

- High epithermal detection efficiency.

  (A 2 mm thick glass has an efficiency of 60% for 0.5 Å neutrons)

- High instantaneous count-rate capability.

  (The scintillation light decays in less than 1 μs)

- Virtually no parallax.

  (The glass scintillator is typically only 1-2 mm thick).

- Nearly windowless enclosure.

  (The window consists merely of a light-tight aluminum foil and the powder reflector)

- Versatile geometric configuration.

  (It can be made round or rectangular, and it can have a scintillator with a neutron-through hole in the center)

- Simple and rugged construction.

  (It is a compact device which requires minimal machining and has no

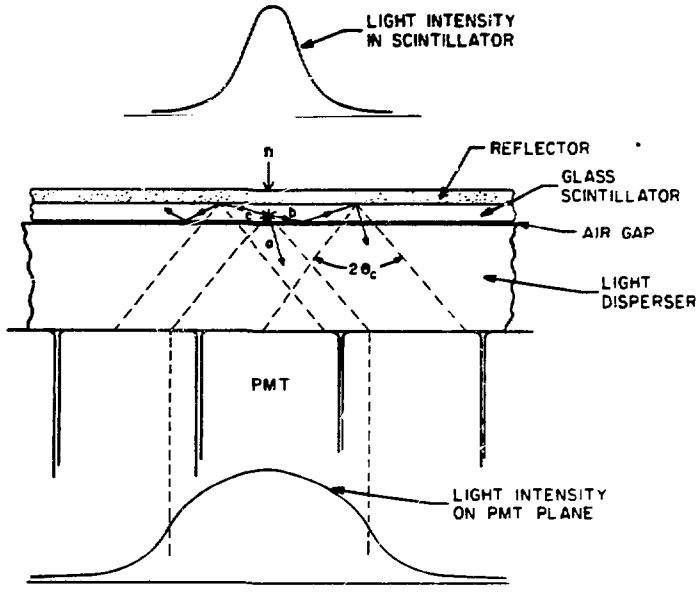

Fig. 4. Optical system of detector. The air gap produces a critical refraction angle (θ_c=40°) beyond which light undergoes total internal reflection. On top is shown the light distribution exiting the glass and on bottom that transmitted to the PMT plane. The latter is characterized by a cutoff which corresponds to the light cone. Thus, the air gap in effect concentrates the light on the PMTs nearest to the scintillation.

3. SPATIAL RESOLUTION CONSIDERATIONS

Insight into the factors affecting the spatial resolution can be gained by examining the optical system of the detector shown schematically in Fig. 4. The operation of the system may be described by following the light paths due to a neutron (n) absorption in the glass scintillator. The air gap produces a critical refraction angle (θ_c=40°) beyond which light undergoes total internal reflection. Thus the light received by the PMTs is limited to a cone consisting of rays, such as a, with an incident angle less than θ_c. Light rays having an incident angle greater than θ_c, such as b, are totally reflected at the air gap and in turn at the diffusing reflector. Those reflected rays having an incident angle of less than θ_c will then be transmitted as shown. Light rays whose initial direction is upwards, such as c, may be reflected several times before they are transmitted to the PMTs. The light intensity distribution produced as a result of this process is plotted above the reflector. The width of the distribution shown is wider, relative to the PMT diameter, than it really is due to the thickness of the scintillator which is also shown exaggerated for the sake of clarity. The light intensity distribution produced on the PMT plane is characterized by a cutoff defined by the light cone. Thus, the air gap in effect concentrates the light on the PMTs nearest to the scintillation. The sharpness of the light cutoff is a function of the scintillator

thickness. As the thickness increases, the lateral spread of the light in the scintillator increases and the cutoff becomes softer.

For each neutron detected the coordinates of the centroid X_o, Y_o are calculated by the readout electronics (Fig. 1). For example, for the X coordinate the centroid X_o is approximated by dividing the sum of the moments $X_i N_i$ by the photoelectron yield in all the PMTs $\sum_i N_i$. Thus,

$$X_o = \frac{\sum_i X_i N_i}{\sum_i N_i} \tag{1}$$

where X_i is the X coordinate of the ith PMT center. The spatial resolution is determined by the statistical spread of the centroids resulting from neutron interactions at any single point. If $\bar{X}_o$ is the mean centroid the FWHM, as determined from error propagation considerations, is

$$\Delta\bar{X}_o = \frac{2.35}{\sqrt{\sum_i N_i}} \sqrt{\sum_i \left[(X_i - \bar{X}_o)^2 \frac{N_i}{\sum_i N_i} \right]} \tag{2}$$

where $X_i - \bar{X}_o$ and $N_i / \sum_i Ni$ are the ith PMT moment arm and fractional photoelectron yield, respectively.

The three factors which determine the spatial resolution are:

(a) PMT Face Dimension

In a closely packed PMT array, $X_i - \bar{X}_o$ is directly proportional to the face dimension of the PMTs. A reduction in this dimension results in a proportionate decrease in the FWHM as long as the PMT is large compared with the width of the light distribution exiting the scintillator (Fig. 4) which is the ultimate limiting parameter.

(b) Total Photoelectron Yield

The photoelectron yield of all the PMTs is represented by $\sum_i N_i$ which has an

inverse square root effect on the FWHM. The photoelectron yield is determined by the following parameters:

1) Scintillator Light Output

This quantity varies with the composition of the glass scintillator as shown in Table 1. For example, type GS2 glass contains less ^{6}Li and has higher light output.

TABLE 1. Glass Light Output

Glass Scintillator*	^{6}Li % Wt	Relative Light Output†
GS20	7	1.0
GS2	2	1.25

† Based on measurements of one sample.

The amount of ^{6}Li in the glass determines its neutron absorption efficiency. This was calculated for 1 and 2 mm thickness as shown in Table 2. At thermal energies (1.8 Å), the efficiency of type GS2 glass is significantly lower than that of type GS20, but at longer wavelengths it is comparable.

TABLE 2. Glass Detection Efficiency

λ	E	GS20* Thickness		GS2* Thickness	
(Å)	(meV)	0.1 cm	0.2 cm	0.1 cm	0.2 cm
1.8	25.2	0.82	0.97	0.39	0.63
5	3.3	0.99	1.0	0.75	0.94
8	1.3	1.0	1.0	0.88	0.99

* Levy West Laboratories, Middlesex, U.K.

2) Optical Transmission from Scintillator to PMTs.

Transmission losses reduce the amount of light reaching the PMT plane. Most of the losses are due to absorption in the reflector. Approximately 12% of the photons produced in a scintillation are within a solid angle defined by $2\theta_c$ (Fig. 4) and are transmitted directly to the PMTs. Most of the remaining ones reach the reflector where the majority of them are reflected but some are absorbed. This process repeats several times. Of the photons that are reflected within $2\theta_c$, some are absorbed in the glass scintillator and some in the disperser. A total loss of ~25% was observed; this includes ~4% per mm of glass thickness. Losses in the disperser were not measured but are believed to be small.

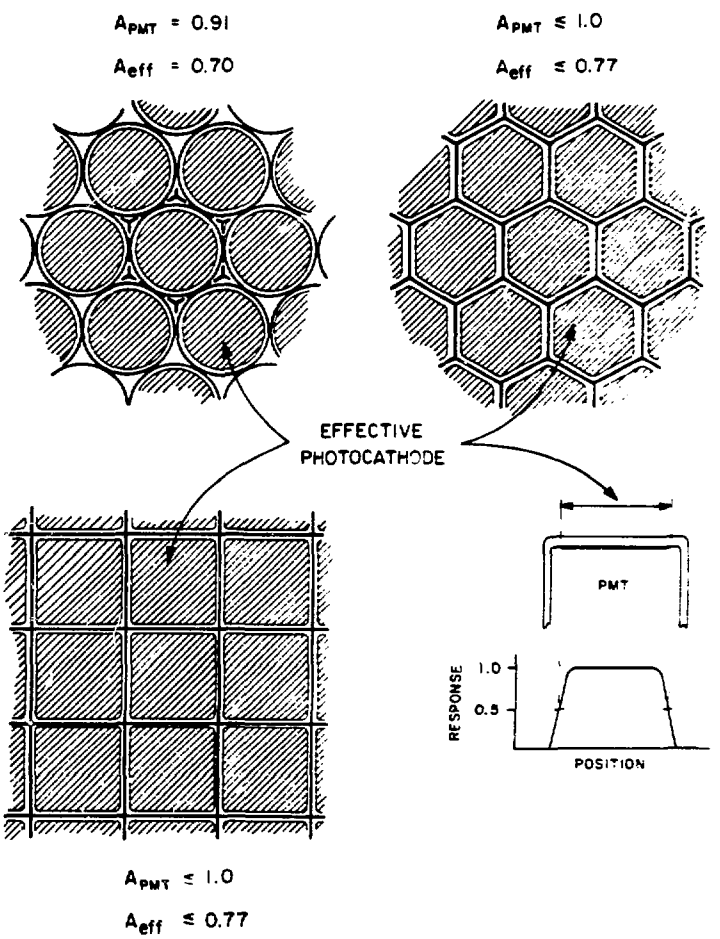

Fig. 5. Configuration of detector with different shape photomultiplier tubes (PMTs). PMT coverage of a unit detector cell is given by A_{PMT} and photocathode coverage by A_{eff}. Note that A_{eff} is significantly smaller than A_{PMT}.

3) Photocathode coverage of PMT plane.

The fraction of the photons reaching the PMT plane and are incident on the photocathode is determined by the shape of the PMT (Fig. 5). Considering a

hexagon or a square as unit cell of the plane, a hexagonal or square PMT would cover the entire cell ($A_{PMT} = 1$) were it not for the rounded corners. A round PMT covers only 91% of the hexagonal cell. For any given PMT, the photocathode covers only a fraction of its face. This fraction, as defined in Fig. 5 (lower right), was measured in an array of 19 round PMTs to be 0.70. Since the area A_{PMT} for a hexagonal and square PMT is ~10% larger, one can assume that the effective photocathode area A_{eff} will also be ~10% larger than for round PMTs. From the above considerations it is apparent that the effective photocathode area in all PMTs is significantly less than the area of the PMT face.

4) PMT Efficiency

Ultimately the photoelectron yield is a direct function of the photocathode quantum efficiency and the photoelectron collection efficiency of the first dynode.

(c) PMT Fractional Photoelectron Yield

The fractional yield $N_i / \sum_i N_i$ is determined by the light distribution on the PMT plane. For the purpose of centroid determination the light need only fall on two PMTs in each of the X and Y directions. A wider distribution than that merely results in broadening the FWHM. PMTs that are remote from the scintillation point have long moment arm $X_i - \bar{X}_o$ and receive only a small fraction of the total light. Their relative contribution to the centroid determination [Eq. (1)] is directly proportional to the moment arm whereas their relative contribution to the FWHM [Eq. (2)] is proportional to the square of the moment arm. Since large uncertainties are associated with the signals from these PMTs, the remote PMTs contribute, relative to the nearby PMTs, more to the uncertainty of the centroid than to its determination. Thus, it is desirable to confine the light to the PMTs nearest to the point where the scintillation occurred. The air gap (Fig. 4) is introduced for that very purpose. It limits the light spread to a reasonably well defined cone which can be further constricted by other means (5,6). The extent of the cone opening is

determined by the thickness of the disperser. The light distribution, and in turn the disperser thickness, also affects the detector linearity. Thus, the thickness of the disperser is selected for the optimum combination of resolution and linearity and is typically 1.5 times the radius of the PMT.

4. SPATIAL RESOLUTION MEASUREMENTS

In order to determine how different components of the detector affect its resolution, we measured the FWHM by several different methods.

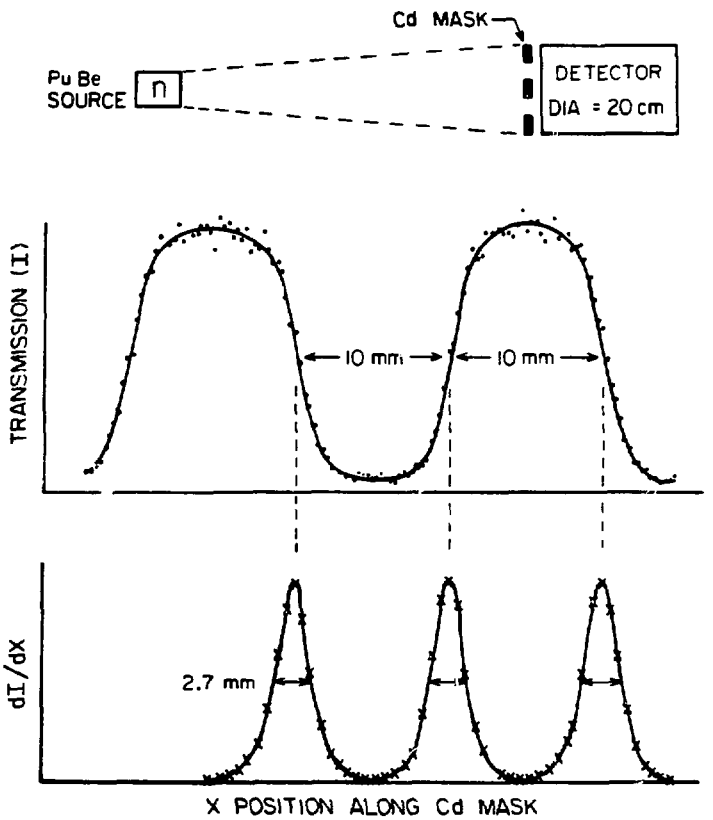

Fig. 6. Spatial resolution obtained by flooding a Cd bar mask with thermal neutrons (top). The measured step response is shown in the middle and the line response, as obtained by differentiation of the step, is shown on the bottom. Nonuniform response in the scintillator and/or readout circuits would increase the FWHM.

(a) Neutron Response

The step-function response of the detector was measured by placing a cadmium mask on the detector face and flooding it with thermalized neutrons from a PuBe source situated 2 m from the detector as shown in Fig. 6 (top). The mask consists of 10 mm wide Cd bars spaced 10 mm apart. The step response obtained from the flood, in the center region of the detector, is shown in the middle (Fig. 6). Differentiation of the step response gives the line response function as shown on the bottom.

This method of measuring the resolution has an advantage over the slit method used before (1). It gives the intrinsic FWHM of the detector directly rather than the convoluted detector-slit response.

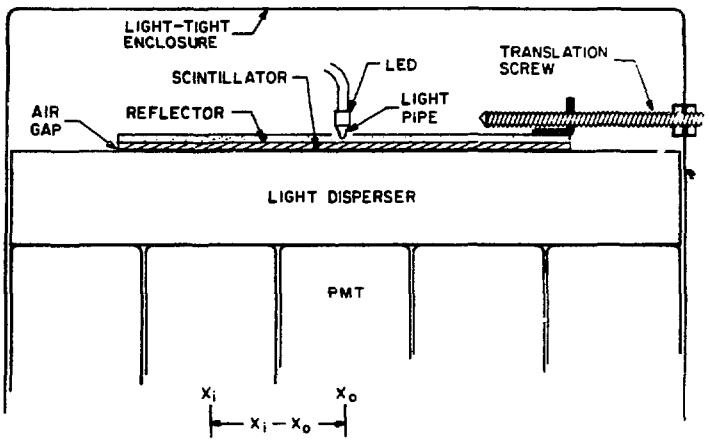

Fig. 7. Test setup using a light emitting diode (LED) for measuring spatial resolution and light yield. Translation screw provides the means for calibrating the spatial response in mm/channel. Nonuniformity in scintillator does not affect the measured FWHM. Since the LED output conforms to Poisson statistics, the light yield is obtained from the pulse height resolution.

(b) Light Response

In order to separate any possible broadening intrinsic to the scintillator, such as nonuniform scintillator response, we designed a test setup for measuring the FWHM with a light-emitting diode (LED) as shown in Fig. 7. The light from the LED is diffused through the reflector, to simulate the scintillator output. The light wavelength need not be identical to that of scintillator as the intensity is adjustable. The translation screw provides the means for calibrating the spatial response in mm/channel.

This method of measuring the resolution is particularly useful during the development and testing stages of the detector as it is fast and convenient. The effect on resolution of component changes or design modification can be determined quickly and reliably with the LED test setup.

(c) Parameter Measurements

Resolution determination from the parameters which control it provides valuable insights into the detector performance. This determination is achieved by measuring the individual parameters which make up Eq. (2): $N_i/\sum_i N_i$, $X_i - \bar{X}_o$, and $\sum_i N_i$. The

measurements of these parameters were made with the test setup shown in Fig. 7. The LED was placed in the center of a detector consisting of a hexagonal array of 19 round PMTs (51 mm dia.) and 1 mm thick GS20 ^{6}Li glass. For each ring of PMTs the fractional photoelectron yield $N_i / \sum_i N_i$ was determined from the relative pulse height, and the moment arm $X_i - \bar{X}_o$ from the array geometry (Fig. 5, upper left). The total photoelectron yield $\sum_i N_i$ was determined by two independent methods.

1) Yield Measurement with a LED

Since the LED output follows Poisson statistics, the fractional pulse height resolution R is 2.35 $(\sum_i N_i)^{-1/2}$, and the photoelectron yield is

$$\sum_i N_i = \left(\frac{2.35}{R}\right)^2 \quad \text{pe/n} \tag{3}$$

where R is the resolution in the E signal (Fig. 1). When the LED was adjusted to produce an E signal equal in amplitude to that of a neutron produced scintillation, the yield according to Eq. (3) was 800 photoelectrons per neutron (pe/n).

2) Yield Measurement with a Scintillator

The light output due to neutrons from a sample of GS20 glass optically coupled to a single PMT was compared with that from NaI(Tl) due to γ rays using the same PMT under the same conditions. The pulse height due to neutrons in the glass was found to be 126 keV γ-ray equivalent. Assuming the absolute scintillation efficiency of NaI(Tl) to be 13%, the light output of the glass, using an amplifier with 1 μs peaking time, is 5300 photons per neutron.

Comparison of the pulse height obtained with an air-gap between the sample glass and a single PMT and that obtained when the glass is coupled to the PMT with an optical compound is a measure of the scintillator-to-PMT

transmission efficiency. From several measurements we observed that for the "air coupled" case the pulse height is approximately 75% of that for the optically coupled one. This reduction is believed to be largely due to the losses in the reflector.

The fractional coverage of a hexagonal detector cell by the photocathode was measured in the array of 19 round PMTs to be 0.7 (Fig. 5, upper left). The typical quantum efficiency for the PMTs is specified to be 0.28. The total photoelectron yield $\sum_i N_i = 780$ photoelectrons per neutron is obtained from the product of the light output, transmission efficiency, photocathode coverage, and quantum efficiency. The yield determination by the two methods is thus seen to be in good agreement.

The resolution values obtained in the above three measurements are listed in Table 3.

TABLE 3. Resolution Measurements

Method	FWHM (mm)
a) Neutron Response	2.7
b) Light Response	2.3
c) Parameter Measurements	1.9

The resolution values in b) and c) are within ±10%. Both were measured at a single point in the center of the detector. The resolution obtained in a) is a summation of several points in the Y direction. The resolution in a) would be expected to be the same as in b) and c) were it not for possible spatial distortion and/or nonuniform response of the scintillator. These would broaden the FWHM in a) and thus may account for part or all of the discrepancy with the lower values obtained in b) and c).

5. CONCLUDING DISCUSSION

The high cost of producing neutrons makes their efficient utilization essential, hence the requirement for a detector not only with high detection efficiency but also with high spatial resolution. The considerations and measurements covered in the previous sections, suggest various means for improving the resolution. The most obvious and direct approach is to use smaller PMTs. A reduction in the face dimension translates directly into a corresponding reduction in the FWHM. However, this approach increases the number of components required and hence the complexity and expense of the detector. For example, a 20 cm dia. scintillator requires 19 PMTs of 51 mm dia. or 61 PMTs of 28 mm dia. Thus, to improve the resolution by not quite a factor of 2, requires more than 3 times the number of PMTs and preamplifiers. This is to be expected when considering that a resolution area element is proportional to the square of the PMT separation distance. A modest improvement can be achieved by using hexagonal (or square) PMTs instead of round ones. These have approximately 10% larger area and hence higher photoelectron yield which may improve the resolution by ~5%.

The highest potential for improving the resolution lies in the scintillator. ^{6}Li glass is a poor scintillator compared (1) with NaI(Tl). The scintillation efficiency due to neutrons in type GS20 glass is only 2.6% of that due to γ rays in NaI(Tl). Glass type GS2 has approximately 25% higher light output and therefore should improve the resolution by 12%. However, for neutrons of thermal energies and above, GS2 glass has lower detection efficiency. One can compensate for that by using thicker glass, but that would offset its advantage. We observed 5-10% broadening in the FWHM when the glass thickness is increased from 1 mm to 2 mm even though the disperser thickness is optimized accordingly.

Kurz and Schelten (7) considered the substitution of the ^{6}Li glass scintillator with ^{6}LiI(Eu). They found that light output of ^{6}LiI(Eu) is 12 times higher than that of ^{6}Li glass. This could improve the spatial resolution by a factor of $\sqrt{12} = 3.5$ which would bring it into the range of 0.5-1 mm using 51 mm dia. PMTs. The linear attenuation coefficient Σ of ^{6}LiI(Eu) is ~17 cm^{-1} which is comparable

to that of GS20 glass. The thickness required for a given efficiency would therefore be the same for the two scintillators. While the higher light output makes the ^{6}LiI(Eu) very attractive, it has also some shortcomings. Having a higher Z than glass, it is somewhat more sensitive to γ rays. Gamma rays are also produced by the neutron capture in iodine. The light decay constant is 1.4 μs which is considerably longer than that of glass (1). Although price is not an inherent property, one cannot overlook the fact that at present the cost of ^{6}LiI(Eu), per unit area, is 2-3 times that of ^{6}Li glass. Notwithstanding the above shortcomings, the use of ^{6}LiI(Eu) merits further investigation as there are undoubtedly applications where the advantage of high spatial resolution outweighs the above disadvantages.

Short of finding a more efficient scintillator, the photoelectron yield can be increased by reducing the light losses. Nearly 20% of light appears to be lost in the reflector, hence, investigating different reflecting surfaces might well be fruitful.

ACKNOWLEDGMENTS

Discussions with G.H. Lander were stimulating and useful. This work was performed under the auspices of the U.S. Department of Energy.

REFERENCES

1. Strauss, M.G., Brenner, R., Lynch, F.J. and Morgan, C.B. (1981). IEEE Trans. Nucl. Sci. NS-28 (1), 800-806.

2. Anger, H.O. (1958). Rev. Sci. Instr. 29. 27-33.

3. Brenner, R., Chou, H.P., Strauss, M.G. and Winiecki, A.L. (1982). IEEE Trans. Nucl. Sci. NS-29 (1), 207-211.

4. Schultz, A.J., Teller, R.G., Williams, J.M., Strauss, M.G. and Brenner, R. (1982). Trans. Am. Cryst. Assoc. 18.

5. Kulberg, G.H., van Dijk, N. and Muehllehner, G. (1972). J. Nucl. Med. 13, 169-171.

6. Seeger, P.A. (1982). Proceedings of this workshop.

7. Kurz, R. and Schelten, J. (1982). Proceedings of this workshop.

DISCLAIMER